https://doi.org/10.48048/tis.2022.5699

An Efficient Control Scheme Based on PLL Integrated PI Controller for Grid-connected Solar Photovoltaic Systems

Sabisha Sureshbabu and Aseem K*

Department of Electrical and Electronics Engineering, LBS College of Engineering, Kasaragod, Kerala, India

(*Corresponding author's e-mail: aseem@lbscek.ac.in)

Received: 8 May 2021, Revised: 26 July 2021, Accepted: 8 August 2021

Abstract

The market for solar energy is growing these days, thanks to recent developments in Photovoltaic (PV) systems. The integration of solar energy to the grid is required for its optimum utilization. A novel control of a single stage 3 phase grid connected solar inverter is presented in this paper. A PV array, Voltage Source Inverter (VSI) for converting dc to ac, and a filter that connects it to the grid are the major components of the proposed system. The inverter output is regulated with respect to the grid using Synchronous Reference Frame (SRF) control. A 3-phase Phase Locked Loop (PLL) is used to lock the grid frequency and phase in relation to inverter output voltage. The Perturb and Observe (P&O) algorithm is used to obtain the reference voltage corresponding to the maximum PV power. To remove the high frequency harmonics, the inverter output is combined with an LCL filter. The dynamic performance of the proposed system under the number of stochastic environmental conditions are validated using MATLAB Simulink platform.

Keywords: Grid connected VSI**,** P&O based MPPT, Phase locked loop, PI controller

Introduction

Total energy consumption is increasing every day, and by 2050, it would have increased by nearly twofold. This demand can be met with a variety of resources, and in the coming years, it will need to be rapidly increased. Traditional energy sources, such as fossil fuels, are unsuitable because they pollute the environment and release greenhouse gases. As a result, renewable energy technology is rapidly expanding to meet future energy demand while remaining pollution-free. Because of its widespread availability, solar energy is the most commonly used renewable energy source. Because of factors such as improved solar cell efficiency, manufacturing technology advancements, and economic scale, solar energy demand has risen in recent years. Grid-connected renewable energy projects face a range of issues due to their varying generation speeds, one of which is grid utility compatibility. To solve this problem, these systems have some form of interface that helps to inject synchronized power into the grid.

Khawla *et al.* [1] proposes a low-voltage ride-through control strategy is for a three-phase grid-connected photovoltaic (PV) system. A flexible control strategy is developed for the proposed system. Both in regular mode and grid fault mode, it controls PV converter operations (symmetrical and asymmetrical grid voltage sag). Sufyan *et al.* [2] deals with the major issues of increasing penetration level and integration of a PV system into the grid, as well as the network's reliability. As a result, grid operators are issuing grid codes to low-voltage networks suffering grid faults. The 3 main forms of control strategies are proposed to maintain the power factor, constant active power control, and constant reactive power control. A 3-phase nonlinear control system for PV generators connected to the grid is given in [3-4]. The controller is built using the Lyapunov method, which is based on the system's nonlinear model. The active and reactive power management of a 3-phase grid-connected photovoltaic device is considered in [5]. Renewable energy sources may be used repeatedly because they are self-renewing [6]. The dependability and accuracy of these systems are still being evaluated. A DC-DC step up converter (boost converter) with maximum power point tracing (MPPT) is used to pull the full power from the sun and send it to the grid [7]. With an advanced control strategy, a 3-phase grid-connected photovoltaic generation system with no boost converter feeding linear or non-linear load is presented in [7]. The controller is built using the Back stepping technique, which is based on a model of the system in

the dq0 axis. The PV system is set to run at near maximum power and acts as an active filter that can compensate for harmonics. Three-phase grid-connected photovoltaic device that maps the PV array's maximum power point using perturb and observe algorithm is detailed in [8-10]. The d-q transformation and sinusoidal PWM technique, as well as grid synchronization conditions, are presented for the inverter control system in [11,12]. Grid-connected PV systems must extract maximum power from PV arrays and inject an almost harmonic free sinusoidal current into the grid [13]. Using a 3-phase architecture for high-power applications leads the following advantages from the inverter's perspective [14]:

(1) The amount of stress on the inverter switches is reduced.
(2) Increases the output frequency of the output current to reduce the size of the output filter.
(3) The size and rating of reactive parts have been decreased.
(4) Creating a loss distribution with a uniform distribution.

Figure 1 depicts a 3-phase single-stage grid-connected PV system. PV array integration with the grid causes a slew of issues, including power quality loss, grid instability and power outages. Harmonic mitigations are important in a grid-connected PV system. PV array size can be increased while power efficiency is maintained using PID controllers. Synchronous frame synchronization is proposed along with dc voltage and d-q axis current control.

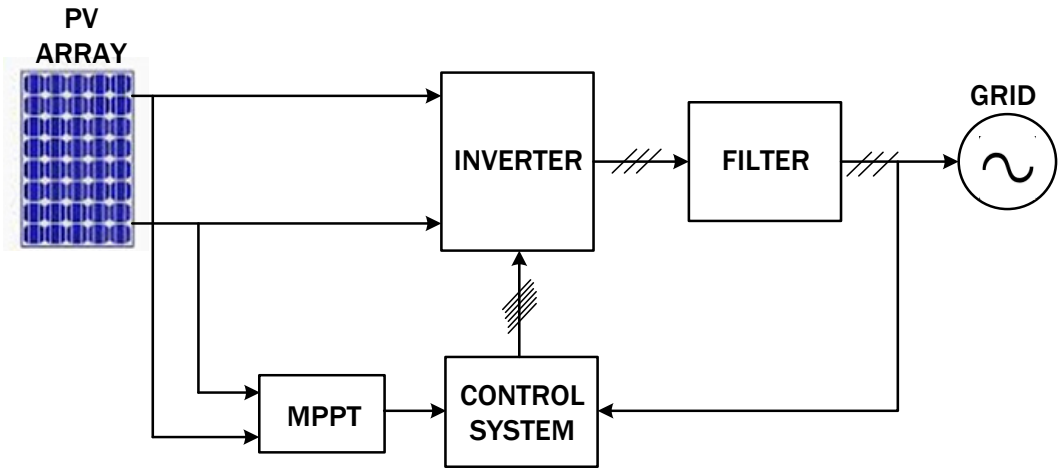

Figure 1 Schematic diagram of grid-connected PV system.

Modelling of PV system

The electrical equivalent circuit model of a PV cell is shown in **Figure 2**. A photovoltaic module is made up of solar cells that are connected in series and parallel. A light-generating current source, a diode, and series and parallel resistance are the main components of the analog circuit. The following are the characteristic equations for the current and voltage of a PV cell:

$$I_{pv} = I_{ph} - I_0 \left\{ exp\left[\frac{q}{nKT}\left(V_{pv} + I_p R_s\right)\right] - 1 \right\} - \left[\frac{V_{pv}+I_p R_s}{R_p}\right] \quad (1)$$

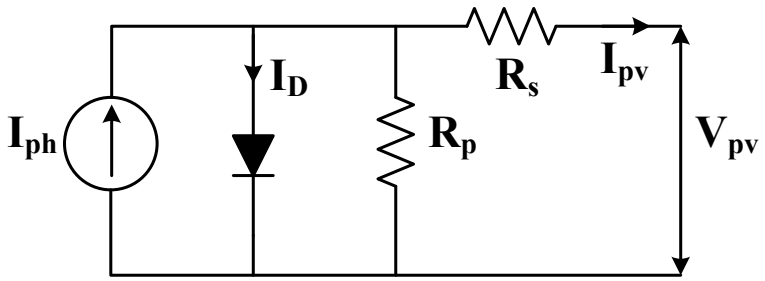

Figure 2 Equivalent circuit of a PV cell.

I_{pv} - the PV cell output current (A), I_{ph} - light generated current (A), I_0 - cell reverse saturation current (A), V_{pv} - PV cell output voltage (V), n - deviation factor from the diode, T - cell temperature (K), K - Boltzmann's constant = $1.3807 \times 10^{-23} J/K^4$, q - electronic charge = $1.6022 \times 10^{-19} C$, R_s - resistance in series (Ω) and R_p - resistance in parallel (Ω).

Table 1 Specification of the PV panel used for the study.

Parameters	Symbol	Values
Number of cell	N_{cell}	60
Maximum power	P_{MPP} (W)	213.15
Peak voltage	V_{MPP} (V)	29
Peak current	I_{MPP} (A)	7.35
Open circuit voltage	V_{OC} (V)	36.3
Short circuit current	I_{SC} (A)	7.84

Modelling of grid connected solar PV system

A DC-AC inverter has been interfaced between the PV modules and the utility grid in a 3-phase single-stage grid connected PV configuration, as shown in **Figure 3**.

Voltage source inverter

The voltage source inverter operates in the current operated mode. The LCL filter is used to minimize current ripples generated by the switching operation. IGBTs are used as switches at a frequency of 10 kHz. PWM method is used to varying the output voltage by turning on and off a pair of IGBTs at the same time. Here $\boldsymbol{V_{dc}}$ is the input voltage to the inverter.

LCL filter

The harmonics will be pumped into the grid through the inverter's output. The LCL filter separates the high frequency components of the inverter output current. The design component specifications are given in **Table 2**. Eq. (2) gives the inductor's-built value. The reactive power which is supplied by the capacitor (C) at 50 Hz frequency is used to design it. The reactive power is set to 5 % of the rated power and is calculated using Eq. (4).

$$\boldsymbol{L_{max}} = \frac{\boldsymbol{20\,\%\,of\ V_{grid}}}{\boldsymbol{2\pi f \times I_{grid}}} \tag{2}$$

$$\boldsymbol{L_1 = L_2} = \frac{\boldsymbol{L_{max}}}{\boldsymbol{2}} \tag{3}$$

$$\boldsymbol{C} = \frac{\boldsymbol{10\,\%\,of\ P_{rated}}}{\boldsymbol{2\pi \times f \times V_{grid}^2}} \tag{4}$$

where $\boldsymbol{I_{grid}} = \frac{\boldsymbol{P_{rated}}}{\boldsymbol{V_{grid}}}$ - grid current (A), $\boldsymbol{V_{grid}}$ - grid voltage (V) and $\boldsymbol{P_{rated}}$ - rated power in KW.

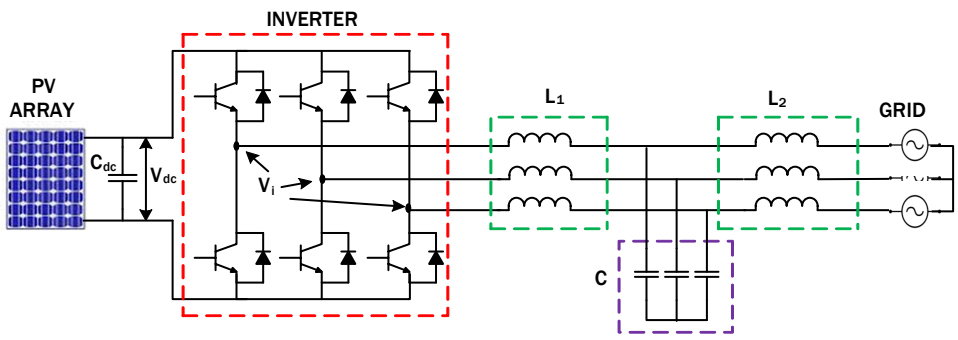

Figure 3 Block illustration of grid-connected PV system.

Table 2 Design parameters.

Parameters	Symbols	Values
Grid Voltage	V_{grid} (V)	400
Grid Current	I_{grid} (A)	250
Rated Power Output	P_{rated} (KW)	100
Grid Frequency	f (Hz)	50
Switching Frequency	f_{sw} (KHz)	10
Inductors	L_1, L_2 (µH)	500
Capacitors	C (µF)	100

The key control used for grid-connected PV system control is the efficient control of inverter which has 2 goals: To regulate the reactive power pumped into the grid and control the active power and to regulate the voltage on the DC bus.

The above 2 objectives are met with the aid of a PI controller, which reduces the output voltage's harmonics. In addition, the MPPT control is used to generate a reference DC bus voltage for proper voltage control.

Perturb and observe (P&O) based MPPT algorithm

The MPPT algorithm is continuously observe the output power of PV array to the perturbation of on array voltage or current. The power of the solar module changes as a result of this disturbance.

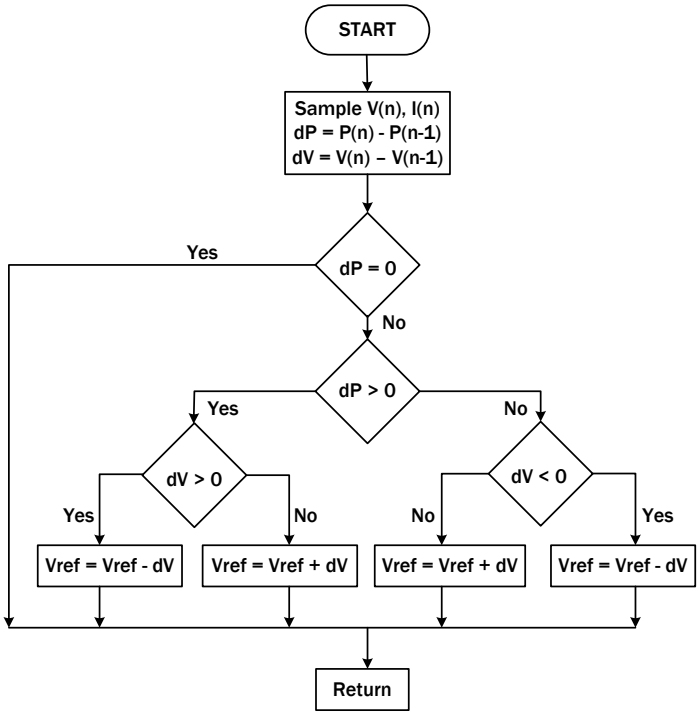

Figure 4 Flowchart of perturb and observe MPPT algorithm.

The flowchart in **Figure 4** illustrates the flow of this algorithm. The PV system's operating voltage is perturbed by a slight increment of V, resulting in a change in power, P. If change in power, dP is positive, the operating voltage must be raised in the same direction as the increment. If dP is negative, on the other hand, the obtained PV operating point shifts away from the MPPT [16,17], requiring the operating voltage to be decreased.

Proposed PLL integrated PI control of inverter

The proposed control strategy is shown in **Figure 5**. It consists of 2 control loops - one for control of DC link voltage and another for d and q-axis current control. In control of DC link Voltage, the reference DC voltage generated by MPPT is compared with measured V_{DC} and a feed forward term is added to the output of DC bus voltage controller, i.e., $\frac{[2/3 P_{pv}]}{V_d}$. Through Parks's transformation, the current loop is performed under DQ rotation reference frame and the power calculated is given by

$$P = \frac{3}{2}\left(V_d I_d + V_q I_q\right) \tag{5}$$

where V_d, V_q are the voltage on D and Q-axis voltage and I_d, I_q are the D and Q-axis current, respectively. The D-axis is oriented along the grid voltage, then, $V_q = 0$. The reference current for D-axis is given by

$$I_{dref} = \frac{[2/3 P_{pv}]}{V_d} \tag{6}$$

where P_{pv} is the active power generated by the solar cell.

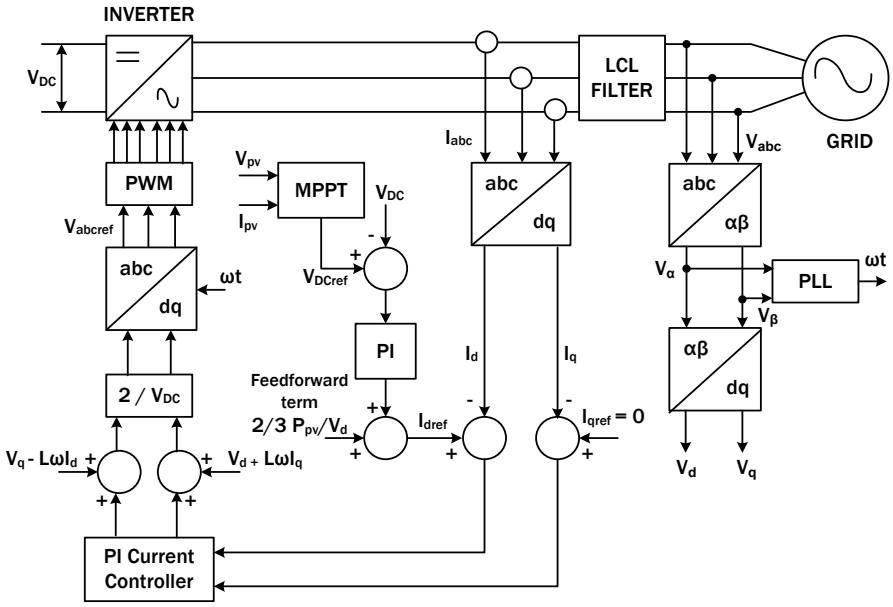

Figure 5 Proposed PLL integrated PI control structure of the 3-phase grid inverter.

The measured inverter current I_{abc} is transformed to I_d and I_q using Parke's transformation. The measured grid voltage V_{abc} is transformed to V_α and V_β. V_α and V_β is again transformed to V_d and V_q using alpha-beta to d-q transformation. The transformed voltage detects phase and frequency of grid, whereas transformed currents are used for control of the grid current. The reference current for active power control is set by DC link voltage, whereas reactive power control reference current is set to 0 value in this case. Then the reference current is compared with actual currents (I_d and I_q). The output of both compensator produces the reference voltages which are again added with the decoupled factor (ωL) to produce the d-q frame modulating signals (M_d and M_q).

Phase locked loop (PLL)

For grid-connected networks, grid synchronization is important. One signal is tracked by another using a PLL technique [15]. It maintains frequency and phase synchronization between the output signal and the reference input signal.

PWM signal generation

In order to minimize input current ripple while maintaining device performance, the inverter switching frequency should be set to 10 kHz. To vary the duty cycle in a dc-dc converter, a triangular wave with a frequency of 10 kHz is compared to the MPPT output to generate the required switching signals.

Controllers parameter

The K_p, K_i and K_d values for the DC link voltage control, PLL and Current controllers are as specified in **Table 3**.

Table 3 Specifications of PID controllers.

Controllers		K_p	K_i
PLL	PID 1	10	50000
DC Link voltage	PID 2	0.25	0.001
d-axis current	PID 3	3.33	5000
q-axis current	PID 4	3.33	5000

Experimental analysis

Under various irradiance and temperature conditions, the performance of PLL integrated PI control of the inverter is carried out. The time domain specification is evaluated and tabulated in **Table 4** under various conditions.

Table 4 Time domain specification of PID controller based on different conditions.

Conditions	Rise-time (µs)	Slew-rate (mv/ms)	Preshoot (%)	Over-shoot (%)	Under-shoot (%)	Settling-time (ms)
Constant irradiance and temperature	910.256	481.081	31.452	28.435	1.965	19.775
Constant irradiance and variable temperature	911.658	482.090	32.542	29.839	1.964	19.885
Variable irradiance and constant temperature	911.642	489.082	32.543	30.493	1.966	19.882
Variable irradiance and temperature	912.752	486.081	32.942	30.564	2.005	20.008

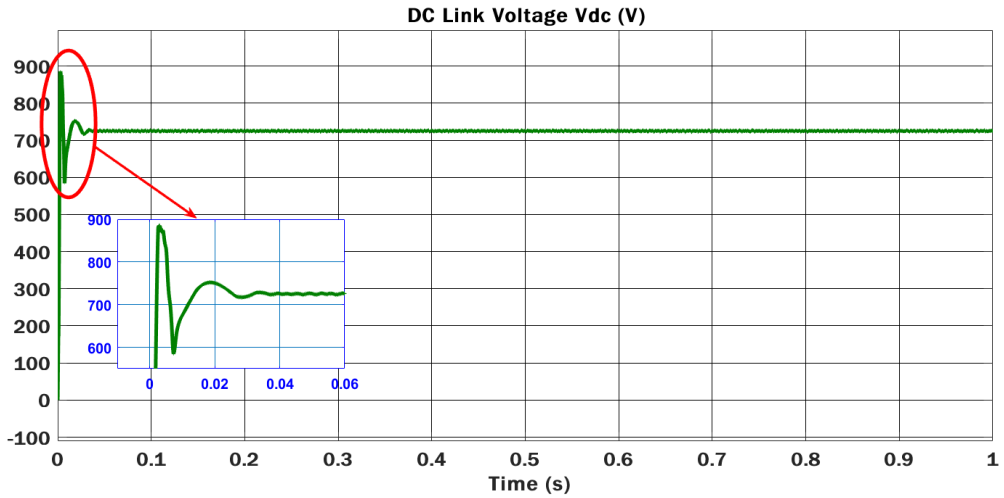

Figure 6 DC Link voltage under constant irradiance and temperature using PLL-PI controller.

Figure 6 provides DC link voltage at 25 ℃ constant temperature and 1,000 W/m^2 irradiance. Here, PLL-PI control gives an overshoot of 28.435 % and an pre-shoot of 32.452 % from t = 0 to 0.02 s. After t = 0.02 s, almost smooth output is obtained with small ripples.

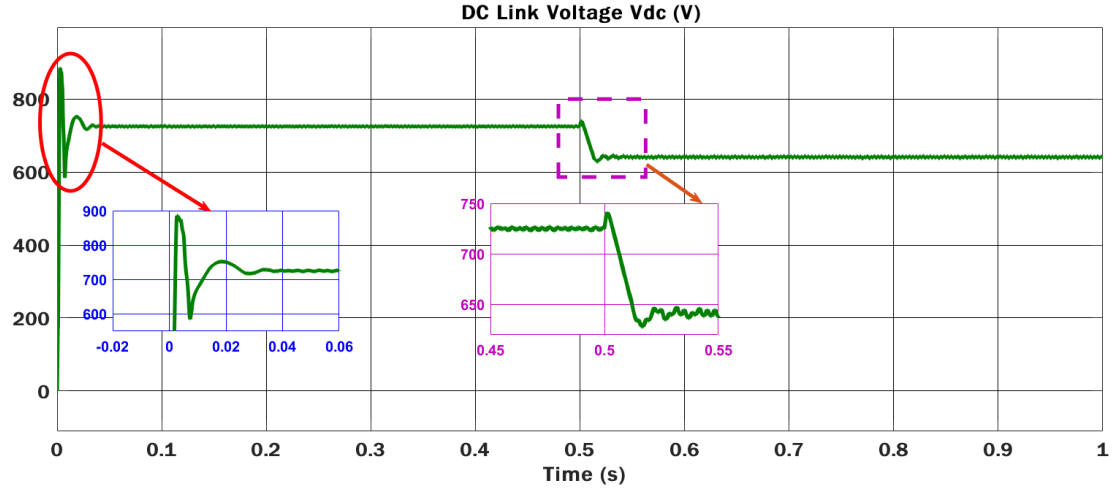

Figure 7 DC Link voltage under constant irradiance and variable temperature using PLL-PI controller.

Figure 7 shows the system under constant 1,000 W/m^2 irradiance and variable irradiance of 25 ℃ at t = 0 to 0.5 s and from t = 0.5 to 1 s, 50 ℃. The transient duration can be perceived between 0 and 0.2 s. Also, there is a dip in voltage from 0.5 to 1 s.

Figure 8 shows the constant 25 ℃ temperature and variable irradiance of 1,000 W/m^2 from t = 0 to 0.5 and 0.7 to 1 s and 400 W/m^2 from t = 0.5 to 0.7 s. The transient occur between t = 0 and 0.2 s and oscillation occurs from t = 0.6 to 0.73 s.

Figure 9 gives the DC voltage under variable temperature of 25 ℃ at t = 0 to 0.5 s and from t = 0.5 to 1 s, 50 ℃ and variable irradiance of 1,000 W/m^2 from t = 0 to 0.5 and 0.7 to 1 s and 400 W/m^2 from t = 0.5 to 0.7 s. Oscillation is little bit high from t = 0.5 to 0.7 s and transient performance is satisfactory.

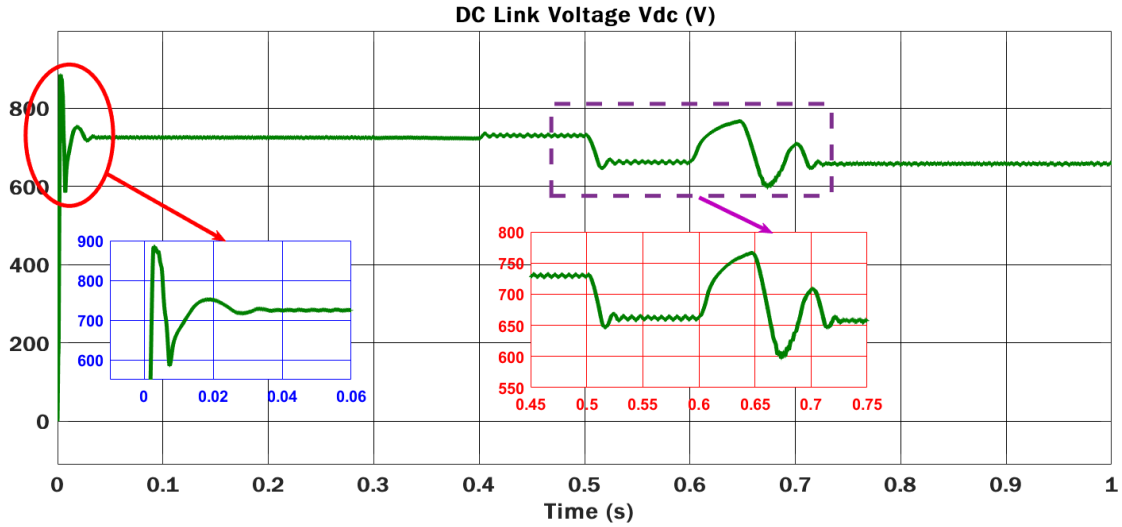

Figure 8 DC Link voltage under constant temperature and variable irradiance using PLL-PI controller.

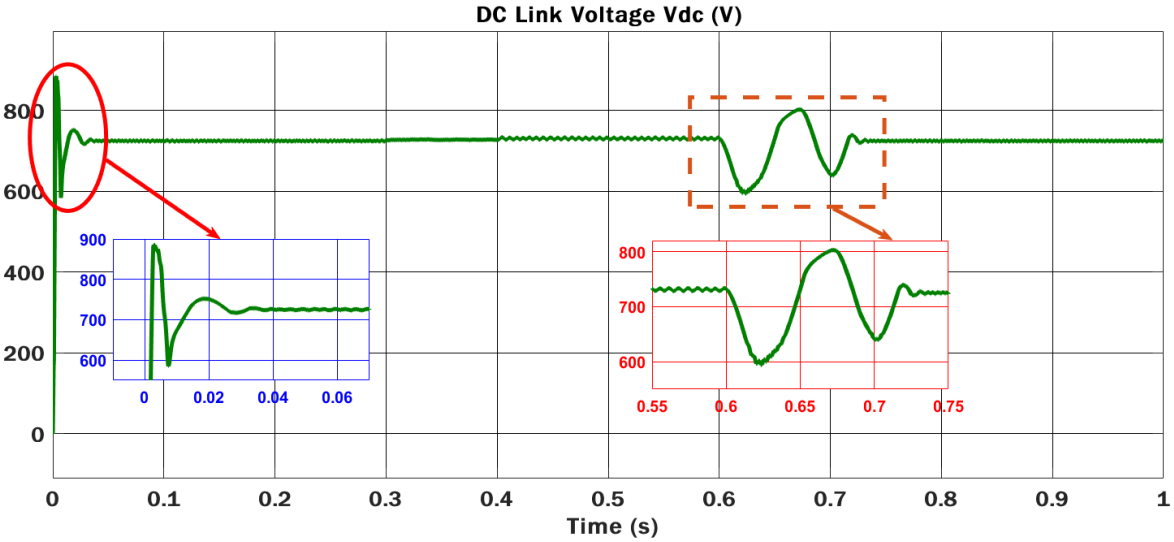

Figure 9 DC Link voltage under variable temperature and irradiance using PLL-PI controller.

Conclusions

The novel PLL integrated PI control strategy for a grid-connected PV system with inverters is introduced. The system is being designed to feed 10 KW of power into the grid. The inverter is controlled to feed active power from the PV panel to the grid through SRF based control strategy. The 3-phase PLL is used to lock inverter frequency and phase with the grid, matching the inverter output frequency to the grid. The dc link voltage is plotted under various temperature and solar irradiance conditions to evaluate the transient performance of the PLL-PI controller. Overshoot, rise time, and settling time are used to quantify the performance of the proposed controller. Despite the fact that grid current harmonics have been decreased, improved controllability is also achieved with the proposed PLL-PI controller.

References

[1] EM Khawla, DE Chariag and L Sbita. A control strategy for a three-phase grid connected PV system under grid faults. *Electronics* 2019; **8**, 906.

[2] M Sufyan, NA Rahim, B Eid and SRS Raihan. A comprehensive review of reactive power control strategies for three phase grid connected photovoltaic systems with low voltage ride through capability. *J. Renew. Sustain. Energ*. 2019, **11**, 042701.

[3] AA Hassan, FH Fahmy, AES Nafeh and HK Youssef. Control of three-phase inverters for smart grid integration of photovoltaic systems. *J. Electric. Syst.* 2022; **18**, 109-31.

[4] P Rai and R Nayak. Modeling & simulation of three phase grid connected solar PV system. *Int. J. Curr. Eng. Tech.* 2018; **8**, 676-81.

[5] PK Sahoo, PK Ray and P Das. Active and reactive power control of three phase grid connected PV system. *Int. J. Smart Grid Green Comm.* 2018; **1**, 275-91.

[6] LK Jisha, Rubeena, S Kavyashree and GR Rashmi. Three phase grid connected photovoltaic power system. *Int. J. Innovat. Res. Elec. Electron. Instrum. Contr. Eng.* 2017; **5**, 51-6.

[7] H Bahri, M Aboulfatah, M Guisser, E Abdelmounim and OS Adekanle. Three-phase grid connected photovoltaic system with active and reactive power control using backstepping method. *In*: Proceedings of the 2nd International Conference on Computing and Wireless Communication Systems, Larache, Morocco. 2017, p. 1-7.

[8] S Pillai and S Thale. Design and implementation of a three phase inverter for renewable energy source with unified control strategy. *Energ. Procedia* 2016; **90**, 673-80.

[9] AH Mollah, GK Panda and PK Saha. Three phase grid connected photovoltaic system with maximum power point tracking. *Int. J. Adv. Res. Elec. Electron. Instrum. Eng.* 2015; **4**, 4637-47.

[10] S Sholapur, KR Mohan and TR Narsimhegowda. Boost converter topology for PV system with perturb and observe MPPT algorithm. *IOSR J. Elec. Electron. Eng.* 2014; **9**, 50-6.

[11] DC Martins. Analysis of a three-phase grid-connected PV power system using a modified dual-stage inverter. *Int. Sch. Res. Not. Renew. Energ.* 2013; **2013**, 406312.
[12] A Refaat, AE Kalas, A Daoud and F Bendary. A control methodology of three phase grid connected PV system. *In*: Proceedings of the Power Systems Conference, South Carolina, USA. 2013.
[13] AS Khalifa and EF El-Saadany. Control of three-phase grid-connected photovoltaic arrays with open loop maximum power point tracking. *In*: Proceedings of the IEEE Power and Energy Society General Meeting, Detroit, Michigan. 2011, p. 1-8.
[14] HS Bae, SJ Lee, KS Choi, BH Cho and SS Jang. Current control design for a grid connected photovoltaic/fuel cell DC-AC inverter. *In*: Proceedings of the Twenty-Fourth Annual IEEE Applied Power Electronics Conference and Exposition, Washington, DC. 2009, p. 1945-50.
[15] SK Chung. Phase-locked loop for grid-connected three-phase power conversion system. *IEE Proc. Elec. Power Appl.* 2000; **147**, 213-9.
[16] A Riccobono and E Santi. Positive feed-forward control of three-phase voltage source inverter for DC input bus stabilization. *In*: Proceedings of the 26th Annual IEEE Applied Power Electronics Conference and Exposition (APEC), Fort Worth, Texas. 2011, p. 741-8.
[17] Y Tian, Z Chen, F Deng, X Sun and Y Hu. Active power and DC voltage coordinative control for cascaded DC - AC converter with bidirectional power application. *IEEE Trans. Power Electron.* 2015; **30**, 5911-25.